

**Odd-parity topological superfluidity for fermions in a bond-centered square optical lattice**Zhi-Fang Xu,<sup>1,2,\*</sup> Andreas Hemmerich,<sup>3</sup> and W. Vincent Liu<sup>4,5,†</sup><sup>1</sup>*Institute for Quantum Science and Engineering and Department of Physics,  
Southern University of Science and Technology, Shenzhen 518055, China*<sup>2</sup>*MOE Key Laboratory of Fundamental Physical Quantities Measurements, School of Physics,  
Huazhong University of Science and Technology, Wuhan 430074, China*<sup>3</sup>*Institut für Laser-Physik, Universität Hamburg, Luruper Chaussee 149, 22761 Hamburg, Germany*<sup>4</sup>*Wilczek Quantum Center, School of Physics and Astronomy and T. D. Lee Institute, Shanghai Jiao Tong University, Shanghai 200240, China*<sup>5</sup>*Department of Physics and Astronomy, University of Pittsburgh, Pittsburgh, Pennsylvania 15260, USA*

(Received 26 March 2017; published 6 November 2017)

We propose a physical scheme for the realization of two-dimensional topological odd-parity superfluidity in a spin-independent bond-centered square optical lattice based upon interband fermion pairing. The  $D_4$  point-group symmetry of the lattice protects a quadratic band crossing, which allows one to prepare a Fermi surface of spin-up fermions with odd parity close to the degeneracy point. In the presence of spin-down fermions with even parity populating a different energetically well-separated band, odd-parity pairing is favored. Strikingly, as a necessary prerequisite for pairing, both Fermi surfaces can be tuned to match well. As a result, topological superfluid phases emerge in the presence of merely  $s$ -wave interaction. Due to the  $Z_2$  symmetry of these odd-parity superfluids, we infer their topological features simply from the symmetry and the Fermi-surface topology as confirmed numerically.

DOI: [10.1103/PhysRevA.96.053607](https://doi.org/10.1103/PhysRevA.96.053607)**I. INTRODUCTION**

Topological superconductivity and its charge neutral analog of topological superfluidity are intriguing forms of topological matter, long sought after in electronic or cold atomic systems [1–15]. Two approaches to topological superconductivity have been taken, either using intrinsic topological superconductors or heterostructures, for example, made of an  $s$ -wave superconductor and a topological insulator [16–18]. As an example, strontium ruthenate [19,20] has been widely discussed as a possible candidate for a topological chiral  $p_x + ip_y$  superconducting phase. The evidence, however, has remained inconclusive. A powerful alternative route towards homogeneous systems showing topological superconductivity is the use of cold atoms [7–15]. In many studies, an interaction involving higher partial waves is required, e.g., a  $p$ -wave interaction induced by spin-orbital coupling. In other cold atom studies this experimentally demanding constraint has been relaxed. For instance, it has been demonstrated as a proof of principle that pairing fermionic atoms from  $s$ - and  $p$ -orbital bands by  $s$ -wave interaction may give rise to the possibility of a topological chiral  $p$ -wave superfluid if the two spin components are loaded into different optical sublattices [12]. The realization of the required spin dependence of the optical lattice potential, however, poses another significant experimental challenge. Particularly, for the widely used fermionic lithium atoms, the small fine-structure splitting practically rules out the possibility of spin-dependent lattices without running into substantial heating.

In this article, we show that topological superfluidity can naturally emerge in a spin- $\frac{1}{2}$  Fermi gas inside an optical lattice by pairing orbital states of odd and even parities.

Our model bypasses the notorious technical complexities that have impeded experiments to date, such as the necessity to engineer synthetic gauge fields, spin-dependent optical lattice potentials, and higher-partial-wave interaction. The two-dimensional (2D) spin-independent optical lattice is derived from a single monochromatic laser beam and provides a  $D_4$  point-group symmetry and a band structure with a quadratic band degeneracy point protected by odd parity. Cooper pair formation only requires  $s$ -wave on-site interactions. Here we summarize the main features and results of our model.

(i) The energy spectrum of the noninteracting part of the model is characterized by two adjacent (second and third) energy bands that are both convex. This is in contrast to an earlier study of an interband pairing mechanism [12] where two adjacent bands generally possess curvatures of opposite sign at the relevant high-symmetry points. We elaborate later that this is very important to well match the Fermi surfaces of the two spin species residing in these two bands.

(ii) The fermionic states close to the Fermi surfaces are mainly composed of highly overlapping orbitals with opposite parities, where the appearance of odd-parity orbitals is guaranteed by tuning the Fermi surface of one spin-component close to the quadratic band crossing.

(iii) Under this condition, our calculation shows that the components of the superfluid order parameter are made from pairings of  $s$ - $p$  and  $p$ - $d$  orbitals. They have odd parity and spontaneously break time-reversal symmetry, thus realizing an odd-parity topological chiral superfluid. Calculations of gapless chiral edge modes further support and classify the topological nature of the phase.

**II. MODEL**

Optical lattices with various unconventional lattice geometries have been implemented in cold atom experiments, such as honeycomb [21], Kagome [22], Lieb [23], and checkerboard

\*xuzf@sustc.edu.cn

†wvliu@pitt.edu

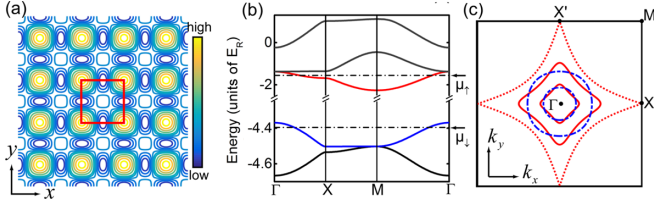


FIG. 1. (a) Contour plot of the optical lattice potential  $V(x, y)$ , with  $V_1 = V_2 = 5 E_R$ , where  $E_R = \hbar^2/(4ma^2)$  is the recoil energy and  $\hbar$  is the Planck constant. The large red (gray) solid square denotes a unit cell of the lattice. (b) Single-particle energy bands along high-symmetry lines. Dotted-dash lines denote the spin-up and spin-down chemical potentials. (c) Fermi surfaces for the spin-up [red (gray) solid line] and spin-down (blue dotted-dash line) components. From inner to outer, 31/32 and 7/8 of the second (third) band are filled by the spin-up (spin-down) fermions for the normal state. A red (gray) dotted line separates two cases where the spin-up Fermi surface encloses the  $\Gamma$  point and the  $M$  point, respectively.

[24,25] lattices. Here, we focus on the 2D optical lattice geometry discussed in Ref. [26] with the potential

$$V(x, y) = -V_1[\cos(k_L x) + \cos(k_L y)] \\ + V_2[\cos(k_L x + k_L y) + \cos(k_L x - k_L y)], \quad (1)$$

illustrated in Fig. 1(a). Here,  $a = 2\pi/k_L$  is the lattice constant. Due to the hybridization among orbitals with different parities and the associated  $D_4$  point-group symmetry, a quadratic band crossing point (QBCP) appears at the  $\Gamma$  point between the third and the fourth energy bands. With arbitrary weak short-range repulsive interaction, the QBCP is unstable towards the formation of topological states, e.g., a quantum anomalous Hall phase [27]. It has been pointed out in Ref. [26] that for  $V_2/V_1 > 1/2$  the potential of Eq. (1) can be readily formed using a single monochromatic laser beam.

In this article, we study a Fermi gas prepared in the optical lattice potential of Eq. (1). In contrast to Ref. [26] we here consider the following three aspects: a spin population imbalance [28,29] such that the Fermi surfaces of spin-up and spin-down components intersect different bands, attractive rather than repulsive  $s$ -wave interaction, and a modified band structure resulting from a different choice of the parameter ratio  $V_2/V_1$ . For the case of  $V_2/V_1 \sim 1$ , the second band is shifted downwards and separated from the third and fourth bands, while the QBCP at the  $\Gamma$  point is retained, as illustrated in Fig. 1(b). Remarkably, both the second and third bands are convex, with their band minima (maxima) both being located at or near the  $M$  ( $\Gamma$ ) point. This feature is important for Cooper pairing. By tuning the spin-up (down) Fermi surface crossing the third (second) band, we are able to obtain well-matched Fermi surfaces, as demonstrated in Fig. 1(c). In contrast to the case of equal spin population, for which both theoretical and experimental studies agree on conventional  $s$ -wave pairing [30–32], we find that appropriate tuning of the spin imbalance can result in the emergence of chiral odd-parity pairing, which is discussed next.

Including the attractive contact interaction, the quasi-2D system is well described by the Hamiltonian

$$\hat{H} = \int d\mathbf{r} \left[ \sum_{\sigma=\uparrow,\downarrow} \hat{\psi}_{\mathbf{r}\sigma}^\dagger (H_0 - \mu_\sigma) \hat{\psi}_{\mathbf{r}\sigma} - U \hat{\psi}_{\mathbf{r}\uparrow}^\dagger \hat{\psi}_{\mathbf{r}\downarrow}^\dagger \hat{\psi}_{\mathbf{r}\downarrow} \hat{\psi}_{\mathbf{r}\uparrow} \right], \quad (2)$$

where  $\mathbf{r} = (x, y)$ ,  $H_0 = -\hbar^2(\partial_x^2 + \partial_y^2)/2M + V(x, y)$ ,  $\mu_\sigma$  is the chemical potential, and  $U > 0$ . In the mean-field framework, we consider only the on-site fermion pairing and define the order parameter as

$$\Delta_{\mathbf{r}} \equiv -U \langle \hat{\psi}_{\mathbf{r}\downarrow} \hat{\psi}_{\mathbf{r}\uparrow} \rangle. \quad (3)$$

Then, the interaction part Hamiltonian becomes  $\hat{H}_{\text{int}} = \int d\mathbf{r} (\hat{\psi}_{\mathbf{r}\uparrow}^\dagger \hat{\psi}_{\mathbf{r}\downarrow}^\dagger \Delta_{\mathbf{r}} + \text{H.c.}) + d\mathbf{r} |\Delta_{\mathbf{r}}|^2/U$ . In the following, we focus on the case of well-matched spin-up and -down Fermi surfaces by tuning the chemical potentials as shown in Fig. 1(c). Therefore, the possibility of Fulde-Ferrell-Larkin-Ovchinnikov states [33–35] is suppressed. It is then reasonable to consider the conventional BCS pairing and assume that the order parameter takes the same periodicity as the optical lattice potential  $V$ . This leads to  $\Delta_{\mathbf{r}} = \sum_{\mathbf{Q}} \Delta_{\mathbf{Q}} \exp[i\mathbf{Q} \cdot \mathbf{r}]$ , where  $\mathbf{Q}$  is the reciprocal lattice vector. To diagonalize the Hamiltonian, we expand the field operator by the Bloch waves as  $\hat{\psi}_{\mathbf{r}\sigma} = \sum_{n\mathbf{k}} \phi_{n\mathbf{k}}(\mathbf{r}) \hat{\psi}_{n\mathbf{k}\sigma}$ , where  $n$  denotes the band index and the Bloch waves can be further expanded by the plane-wave basis as  $\phi_{n\mathbf{k}} = \frac{1}{\sqrt{\mathcal{V}}} \sum_{\mathbf{Q}} \varphi_{n\mathbf{k}}(\mathbf{Q}) \exp[i(\mathbf{k} + \mathbf{Q}) \cdot \mathbf{r}]$ , with  $\mathcal{V}$  being the system volume. Thus, the mean-field Hamiltonian is given by

$$\hat{H}_{\text{MF}} = \sum_{n\mathbf{k}\sigma} [\xi_n(\mathbf{k}) - \mu_\sigma] \hat{\psi}_{n\mathbf{k}\sigma}^\dagger \hat{\psi}_{n\mathbf{k}\sigma} + \frac{\mathcal{V}}{U} \sum_{\mathbf{Q}} |\Delta_{\mathbf{Q}}|^2 \\ + \sum_{n\mathbf{m}\mathbf{k}} (\hat{\psi}_{n\mathbf{k}\uparrow}^\dagger \hat{\psi}_{m, -\mathbf{k}\downarrow}^\dagger \Delta_{n\mathbf{m}\mathbf{k}} + \text{H.c.}), \quad (4)$$

where  $\xi_n(\mathbf{k})$  is the single-particle energy of the  $n$ th band at the crystal momentum  $\mathbf{k}$ ,  $\Delta_{n\mathbf{m}\mathbf{k}} = \sum_{\mathbf{Q}} \Delta_{\mathbf{Q}} (M_{n\mathbf{m}\mathbf{k}}^{\mathbf{Q}})^*$ ,  $M_{n\mathbf{m}\mathbf{k}}^{\mathbf{Q}} = \sum_{\mathbf{K}} \varphi_{m, -\mathbf{k}}(-\mathbf{K}) \varphi_{n\mathbf{k}}(\mathbf{K} + \mathbf{Q})$ , and  $\mathbf{K}$  is the reciprocal lattice vector. Numerically, we take into account the lowest four bands, as they deviate from the upper bands. To obtain the ground state, we use the simulated annealing method to find the global minimum of the grand potential  $\Omega \equiv -\frac{1}{\beta} \ln \text{Tr} \exp[-\beta \hat{H}_{\text{MF}}]$ , accompanied by the self-consistent iteration method [36].

### III. TOPOLOGICAL ODD-PARITY SUPERFLUID

Before showing the ground states, we first analyze the underlying symmetry of the interband pairing for the spin-imbalanced system. To provide a more intuitive picture, we consider two different tight-binding (TB) models [36] to describe the lowest four bands obtained from a numerical plane-wave expansion as shown in Fig. 1(b). The corresponding Wannier functions are chosen as eigenstates of band-projected position operators [37,38]. We find that both TB models describe the numerically determined band structure with excellent precision and generate the same phases [36] when the attractive interaction is turned on. Here, as one example, we consider a TB model involving four orbitals,  $s, p_x,$

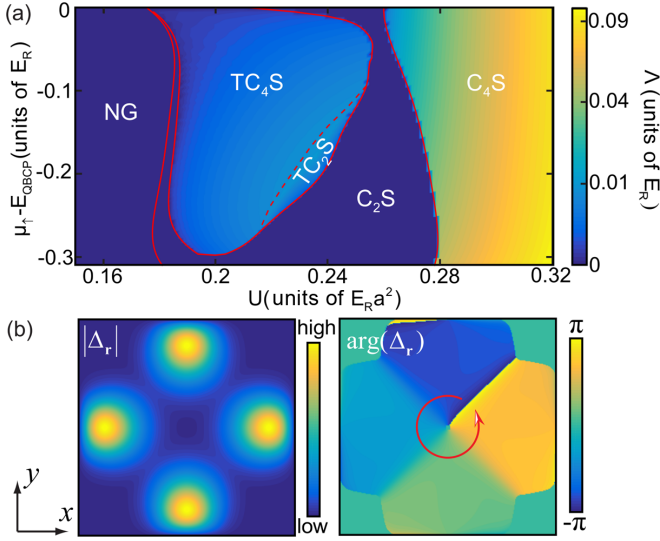


FIG. 2. (a) Zero-temperature ground-state phase diagram by varying the  $s$ -wave interaction and the chemical potentials. Spin-up and spin-down chemical potentials are changed simultaneously to make the enclosed area for two Fermi surfaces equal in the momentum space and  $\mu_{\uparrow} \in [E_{\text{SEP}}, E_{\text{QBCP}}]$ , where  $E_{\text{QBCP}}$  denotes the single-particle energy at the quadratic band crossing, and when  $\mu_{\uparrow} = E_{\text{SEP}}$ , the spin-up Fermi surface is denoted by the red dotted line in Fig. 1(c). Five different phases are denoted by NG,  $\text{TC}_4\text{S}$ ,  $\text{TC}_2\text{S}$ ,  $\text{C}_4\text{S}$ , and  $\text{C}_2\text{S}$ , respectively. The quasiparticle excitation gap  $\Delta$  is shown according to the color gauge. (b) The characteristic spatial distribution of the order parameter in one unit cell for the superfluid phase preserving the fourfold rotation symmetry.

$p_y$ , and  $d_{x^2-y^2}$ , centered at the center of the unit cell denoted by the red square shown in Fig. 1(a). Their corresponding annihilation operators are  $\hat{s}$ ,  $\hat{p}_x$ ,  $\hat{p}_y$ , and  $\hat{d}$ .

When the spin-up Fermi surface is tuned close to the degenerate point ( $\Gamma$  point) between the third and fourth bands, the spin-up fermions close to the Fermi surface are mainly composed of the odd-parity  $p$  orbitals [26,36]. In contrast, close to the spin-down Fermi surface which is tuned to lie near the maximum of the second band, the fermions are mainly composed of even-parity orbitals. All these features can be readily confirmed by diagonalizing the single-particle Hamiltonian [36]. In the weak-coupling limit, the pairing is mainly among fermions close to the Fermi surfaces, and hence Cooper pairing takes place mainly between odd-parity spin-up fermions and even-parity spin-down fermions, leading to odd-parity superfluidity. From a symmetry point of view, the pairing order parameter may largely inherit the  $D_4$  point-group symmetry of the system. The maximally symmetric pairing phase corresponds to locking the phase difference between two degenerate odd-parity orbitals at  $\pm\pi/2$  during pairing, which leads to  $\langle \hat{d}_{\downarrow} \hat{p}_{x,\uparrow} \rangle = \mp i \langle \hat{d}_{\downarrow} \hat{p}_{y,\uparrow} \rangle$  and  $\langle \hat{s}_{\downarrow} \hat{p}_{x,\uparrow} \rangle = \pm i \langle \hat{s}_{\downarrow} \hat{p}_{y,\uparrow} \rangle$ .

Our numerics confirms the existence of the anticipated maximally symmetric odd-parity superfluid phases which are invariant under the combined  $\pm\pi/2$  gauge rotation and the  $C_4$  space-rotation symmetry. The corresponding order parameters are shown in Fig. 2(b). In addition, we find other phases with lower symmetries. Figure 2(a) shows the zero-temperature ground-state phase diagram calculated by the plane-wave

expansion. To facilitate fermion pairing, spin-up and -down chemical potentials are adjusted simultaneously to match the enclosed area of the two Fermi surfaces in momentum space. By varying the value of  $s$ -wave contact interaction between two spin-components and the chemical potentials, we find five different phases.

Because the two Fermi surfaces cross different bands, a finite interaction is needed to get into the superfluid phase. When the interaction is too weak, only a normal gas (NG) phase is obtained. Increasing the interaction gives rise to four different superfluids with odd parity. Two superfluid phases denoted by  $\text{TC}_4\text{S}$  and  $\text{TC}_2\text{S}$  are topologically nontrivial while the others are topologically trivial. Two phases denoted by  $\text{TC}_4\text{S}$  and  $\text{C}_4\text{S}$  spontaneously break the time-reversal symmetry but preserve the  $C_4$  rotation symmetry and are accompanied by a full bulk gap close to the zero energy. We find that both show nonzero orbital angular momenta for the center-of-mass motion of paired fermions, as illustrated in Fig. 2(b) where vortices are found present in each unit cell for both states. This feature is reminiscent of the interaction-driven bosonic chiral superfluid in a checkerboard lattice studied in Ref. [39]. The other two phases, denoted by  $\text{TC}_2\text{S}$  and  $\text{C}_2\text{S}$ , preserve only the  $C_2$  rotation symmetry. The difference between them is that the  $\text{TC}_2\text{S}$  phase also breaks the time-reversal symmetry and shows a full bulk gap, while the  $\text{C}_2\text{S}$  phase preserves the time-reversal symmetry similar to the conventional  $p$ -wave superfluid with a real pairing order parameter and supports gapless excitations.

To determine the topological behavior of the odd-parity superfluid phases, we can rely on the criterion discussed in Refs. [40,41], where the authors show that the topology of the full-gapped odd-parity superconductor—with or without the time-reversal symmetry—can be simply inferred from the Fermi-surface topology, e.g., the number of the time-reversal invariant (TRI) momenta enclosed by the Fermi surface. For the spin-imbalanced system we discussed, the Bogoliubov-de Gennes (BdG) Hamiltonian is given by [36]

$$\mathcal{H}_{\text{BdG}}(\mathbf{k}) = \begin{pmatrix} H_0(\mathbf{k}) - \mu_{\uparrow} \mathbb{1} & \hat{\Delta}(\mathbf{k}) \\ \hat{\Delta}^{\dagger}(\mathbf{k}) & -H_0(\mathbf{k}) + \mu_{\downarrow} \mathbb{1} \end{pmatrix}, \quad (5)$$

where  $H_0(\mathbf{k})$  is a diagonal matrix with elements  $[H_0(\mathbf{k})]_{nn} = \xi_n(\mathbf{k})$  and  $[\hat{\Delta}(\mathbf{k})]_{nm} = \Delta_{nm\mathbf{k}}$ .

As the lattice potential of Eq. (1) is invariant under the  $D_4$  symmetry group, the single-particle band structure exhibits the inversion symmetry  $PH_0(\mathbf{k})P = H_0(-\mathbf{k})$ , where  $P$  is an inversion operator with the inversion center defined at the center of the unit cell denoted by the large red (gray) square shown in Fig. 1(a). Focusing on the odd-parity superfluids shown in Fig. 2(a), the order parameter satisfies  $\Delta_{\mathbf{r}} = -\Delta_{-\mathbf{r}}$ . Further choosing specific relative global phases for the Bloch waves at opposite momenta when calculating  $M_{mn\mathbf{k}}^{\text{Q}}$ , we could make  $\Delta_{mn\mathbf{k}} = -\Delta_{mn,-\mathbf{k}}$ , leading to  $P\hat{\Delta}(\mathbf{k})P = -\hat{\Delta}(-\mathbf{k})$ . We thus find that the BdG Hamiltonian for the odd-parity superfluid has a  $Z_2$  symmetry:

$$\tilde{P}\mathcal{H}_{\text{BdG}}(\mathbf{k})\tilde{P} = \mathcal{H}_{\text{BdG}}(-\mathbf{k}), \quad \tilde{P} \equiv P\tau_z, \quad (6)$$

where  $\tau_z$  is a diagonal matrix with diagonal elements  $[\mathbb{1}, -\mathbb{1}]$ . With this  $Z_2$  symmetry, we can define a  $Z_2$  invariant  $\nu$  for

characterizing the topology of the superfluid [40,41]:

$$(-1)^{\nu} = \prod_{\alpha, \ell (\mathcal{E}_{\ell}(\Gamma_{\alpha}) < 0)} \pi_{\ell}(\Gamma_{\alpha}). \quad (7)$$

where  $\pi_{\ell}(\Gamma_{\alpha})$  and  $\mathcal{E}_{\ell}(\Gamma_{\alpha})$  are the eigenvalues of  $\tilde{P}$  and  $\mathcal{H}_{\text{BdG}}(\Gamma_{\alpha})$  on their common eigenstates at TRI points  $\Gamma_{\alpha}$  and the product over  $\ell$  includes quasiparticle excitations with  $\mathcal{E}_{\ell}(\Gamma_{\alpha}) < 0$ . In the weak-coupling limit, the quasiparticle eigenstates can be approximated by Bloch states of  $H_0$  [40,41]. We thus find

$$(-1)^{\nu} = \prod_{\alpha, n} \bar{p}_n(\Gamma_{\alpha}) \text{sgn}[\mu_{\downarrow} - \xi_n(\Gamma_{\alpha})], \quad (8)$$

where the product over  $n$  covers all bands of  $H_0$  and  $\bar{p}_n(\Gamma_{\alpha}) = p_n(\Gamma_{\alpha})$  if  $[\mu_{\uparrow} - \xi_n(\Gamma_{\alpha})][\xi_n(\Gamma_{\alpha}) - \mu_{\downarrow}] > 0$  and 1 otherwise. Here  $p_n(\Gamma_{\alpha})$  is the eigenvalue of the parity operator for the  $n$ th Bloch states at  $\Gamma_{\alpha}$ . There is a crucial difference from the  $Z_2$  invariant defined in the context of electronic superconductivity [40,41]. Here, due to spin population imbalance, the summation of the occupied spin-up bands and the unoccupied spin-down bands overcompletely covers the complete set of single-particle energy bands. This requires us to consider the parity for the states in between the two Fermi surfaces at TRI points.

The band structure in Fig. 1 shows that the single-particle Bloch states at TRI points in between two Fermi surfaces are not degenerate. Two of them at the  $\Gamma$  and  $M$  points must be even-parity states, because the little groups at the  $\Gamma$  and  $M$  points coincide with the  $D_4$  point group and the odd-parity state should be twofold degenerate [26]. Due to the  $D_4$  symmetry of the lattice, the other two single-particle states at the  $X$  and  $X'$  points should have the same eigenvalue of the parity operator. These lead to  $\prod_{\alpha, n} \bar{p}_n(\Gamma_{\alpha}) = 1$ . We also see that the spin-down Fermi surface encloses only one TRI point. In this sense, we identify that  $\nu = 1$  is for the fully gapped odd-parity superfluid phases, TC<sub>4</sub>S and TC<sub>2</sub>S. That in turn indicates that the two phases are topologically nontrivial. While for the fully gapped C<sub>4</sub>S phase, strong interaction induces a larger pairing order parameter, which changes the structure of excitations leading to different topology as shown in Fig. 3. To prove this conclusion, we directly map out the topological edge excitations by artificially putting periodic domain walls in the system. Figure 3(c) confirms our arguments that the TC<sub>4</sub>S phase is topologically nontrivial. We further confirm that the TC<sub>2</sub>S phase shows similar quasiparticle excitations and is also topologically nontrivial.

We would like to stress that for the weak coupling limit which applies to the topological phases TC<sub>4</sub>S and TC<sub>2</sub>S [36], the mean-field BCS theory should be valid and reliable even for the 2D system we considered. Otherwise, for the strong coupling limit, it is expected to be qualitatively correct based on what is widely known in the study of BCS-BEC (Bose-Einstein condensate) crossover. Also, the strong interaction can undermine the assumption that the order parameter takes the same periodicity as the lattice. As detailed in Ref. [36], the C<sub>4</sub>S phase will be replaced by an even-parity pairing phase.

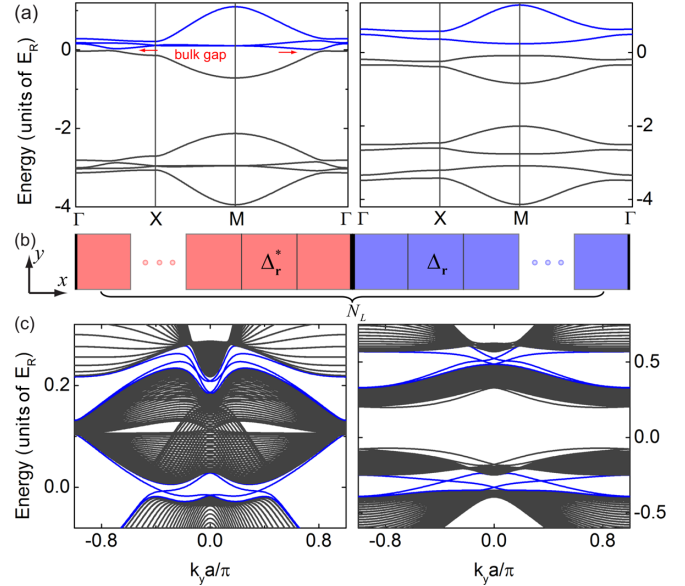


FIG. 3. (a) Quasiparticle excitation spectra for two different odd-parity superfluids, TC<sub>4</sub>S (left panel) and C<sub>4</sub>S (right panel), along the high-symmetry lines in the first Brillouin zone, with  $\mu_{\uparrow} = -1.5497 E_R$  and  $\mu_{\downarrow} = -4.3957 E_R$  and, respectively,  $U = 0.225$  and  $0.315 E_R a^2$ . (b) An enlarged unit cell of a system in the presence of periodic domain walls, which exist at the center and the edges of the enlarged unit cell. Each one contains  $N_L$  unit cells of the optical lattice, which is denoted by solid squares. The pairing order parameters on the left and right parts are the time reversal of each other. (c) Excitation spectra for the system in the presence of domain walls shown in panel (b) with same parameters used in panel (a). Blue (gray) solid lines denote the topological protected excitations at the domain walls. Here, we choose  $k_x = 0$  and  $N_L = 80$ .

#### IV. EXPERIMENTAL REALIZATION AND DETECTION

To generate the desired lattice potential of Eq. (1) in experiments, we merely need to provide a single blue-detuned linearly polarized monochromatic light beam, as described in Ref. [26]. The requirement that  $V_2/V_1 = 1$  can be readily fulfilled. The maximum of the full pairing gap for the topological phases shown in Fig. 2 is about  $0.01 E_R$ , which corresponds to an experimentally feasible temperature scale of 10 nK. The odd-parity superfluids are characterized by the existence of edge states in domain walls or in the edges of a finite system confined in a box trap [42]. By applying spatially resolved radio-frequency spectroscopy [43], the signature of the edge states can be inferred from the local density of states [12].

#### V. CONCLUSION

We study fermion pairing for a spin-imbalanced atomic Fermi gas loaded into a  $D_4$  symmetric spin-independent bond-centered square optical lattice. Topological odd-parity superfluid phases spontaneously emerge from purely  $s$ -wave attractive interactions, in notable contrast to the conventional mechanism of topological superfluidity relying on interaction

of high partial waves. Strong  $s$ -wave interaction can now be routinely realized in cold atomic gases via Feshbach resonances. The key ingredients for the topological superfluid phases presented here are (i) the existence of well-matched Fermi surfaces crossing two neighboring energy bands and (ii) even and odd parities of the fermions close to the spin-up and -down Fermi surfaces, respectively. These necessary prerequisites can be provided in an experimentally easily realizable square optical lattice. Our proposal prevents experimental complexities of previously discussed schemes of topological superfluidity, for example, the necessity of higher-partial-wave interactions, synthetic gauge fields, and spin-dependent lattices.

## ACKNOWLEDGMENTS

The authors would like to thank R. Hulet and D. Stamper-Kurn for stimulating and very helpful discussions. This work is supported by the NSFC (Grant No. 11574100) and the National Thousand-Young-Talents Program (Z.-F.X.) and by the US ARO (Grant No. W911NF-11-1-0230), the AFOSR (Grant No. FA9550-16-1-0006), the Overseas Collaboration Program of the NSF of China (Grant No. 11429402) sponsored by Peking University, and the National Basic Research Program of China (Grant No. 2012CB922101) (W.V.L.). A.H. acknowledges support from the DFG under Contract No. SFB925 and the Hamburg Centre for Ultrafast Imaging (CUI).

- 
- [1] G. E. Volovik, *The Universe in a Helium Droplet* (Oxford University Press, New York, 2003).
- [2] N. Read and D. Green, *Phys. Rev. B* **61**, 10267 (2000).
- [3] C. Nayak, S. H. Simon, A. Stern, M. Freedman, and S. D. Sarma, *Rev. Mod. Phys.* **80**, 1083 (2008).
- [4] C. Kallin, *Rep. Prog. Phys.* **75**, 042501 (2012).
- [5] M. Sato and Y. Ando, *Rep. Prog. Phys.* **80**, 076501 (2017).
- [6] V. Gurarie and L. Radzihovsky, *Ann. Phys.* **322**, 2 (2007).
- [7] C. Zhang, S. Tewari, R. M. Lutchyn, and S. D. Sarma, *Phys. Rev. Lett.* **101**, 160401 (2008).
- [8] M. Sato, Y. Takahashi, and S. Fujimoto, *Phys. Rev. Lett.* **103**, 020401 (2009).
- [9] N. R. Cooper and G. V. Shlyapnikov, *Phys. Rev. Lett.* **103**, 155302 (2009).
- [10] X.-J. Liu, K. T. Law, and T. K. Ng, *Phys. Rev. Lett.* **112**, 086401 (2014).
- [11] A. Bühler, N. Lang, C. V. Kraus, G. Möller, S. D. Huber, and H. P. Büchler, *Nat. Commun.* **5**, 4504 (2014).
- [12] B. Liu, X. Li, B. Wu, and W. V. Liu, *Nat. Commun.* **5**, 5064 (2014).
- [13] S.-L. Zhang, L.-J. Lang, and Q. Zhou, *Phys. Rev. Lett.* **115**, 225301 (2015).
- [14] B. Wang, Z. Zheng, H. Pu, X. Zou, and G. Guo, *Phys. Rev. A* **93**, 031602 (2016).
- [15] Z. Wu and G. M. Bruun, *Phys. Rev. Lett.* **117**, 245302 (2016).
- [16] L. Fu and C. L. Kane, *Phys. Rev. Lett.* **100**, 096407 (2008).
- [17] M.-X. Wang, C. Liu, J.-P. Xu, F. Yang, L. Miao, M.-Y. Yao, C. L. Gao, C. Shen, X. Ma, X. Chen, Z.-A. Xu, Y. Liu, S.-C. Zhang, D. Qian, J.-F. Jia, and Q.-K. Xue, *Science* **336**, 52 (2012).
- [18] J.-P. Xu, M.-X. Wang, Z. L. Liu, J.-F. Ge, X. Yang, C. Liu, Z. A. Xu, D. Guan, C. L. Gao, D. Qian, Y. Liu, Q.-H. Wang, F.-C. Zhang, Q.-K. Xue, and J.-F. Jia, *Phys. Rev. Lett.* **114**, 017001 (2015).
- [19] Y. Maeno, H. Hashimoto, K. Yoshida, S. Nishizaki, T. Fujita, J. G. Bednorz, and F. Lichtenberg, *Nature (London)* **372**, 532 (1994).
- [20] A. P. Mackenzie and Y. Maeno, *Rev. Mod. Phys.* **75**, 657 (2003).
- [21] P. Soltan-Panahi, J. Struck, P. Hauke, A. Bick, W. Plenkers, G. Meineke, C. Becker, P. Windpassinger, M. Lewenstein, and K. Sengstock, *Nat. Phys.* **7**, 434 (2011).
- [22] G.-B. Jo, J. Guzman, C. K. Thomas, P. Hosur, A. Vishwanath, and D. M. Stamper-Kurn, *Phys. Rev. Lett.* **108**, 045305 (2012).
- [23] S. Taie, H. Ozawa, T. Ichinose, T. Nishio, S. Nakajima, and Y. Takahashi, *Sci. Adv.* **1**, e1500854 (2015).
- [24] J. Sebby-Strabley, M. Anderlini, P. S. Jessen, and J. V. Porto, *Phys. Rev. A* **73**, 033605 (2006).
- [25] G. Wirth, M. Ölschläger, and A. Hemmerich, *Nat. Phys.* **7**, 147 (2011).
- [26] K. Sun, W. V. Liu, A. Hemmerich, and S. D. Sarma, *Nat. Phys.* **8**, 67 (2012).
- [27] K. Sun, H. Yao, E. Fradkin, and S. A. Kivelson, *Phys. Rev. Lett.* **103**, 046811 (2009).
- [28] M. W. Zwierlein, A. Schirotzek, C. H. Schunck, and W. Ketterle, *Science* **311**, 492 (2006).
- [29] G. B. Partridge, W. Li, R. I. Kamar, Y.-A. Liao, and R. G. Hulet, *Science* **311**, 503 (2006).
- [30] J. K. Chin, D. E. Miller, Y. Liu, C. Stan, W. Setiawan, C. Sanner, K. Xu, and W. Ketterle, *Nature (London)* **443**, 961 (2006).
- [31] H. Zhai and T.-L. Ho, *Phys. Rev. Lett.* **99**, 100402 (2007).
- [32] E. G. Moon, P. Nikolić, and S. Sachdev, *Phys. Rev. Lett.* **99**, 230403 (2007).
- [33] P. Fulde and R. A. Ferrell, *Phys. Rev.* **135**, A550 (1964).
- [34] A. I. Larkin and Y. N. Ovchinnikov, *Zh. Eksp. Teor. Fiz.* **47**, 1136 (1964).
- [35] Y.-A. Liao, A. S. C. Rittner, T. Paprotta, W. Li, G. B. Partridge, R. G. Hulet, S. K. Baur, and E. J. Mueller, *Nature (London)* **467**, 567 (2010).
- [36] See Supplemental Material at <http://link.aps.org/supplemental/10.1103/PhysRevA.96.053607> for additional details on diagonalization of the mean-field Hamiltonian, tight-binding models, and superfluid phases calculated from the tight-binding models.
- [37] S. Kivelson, *Phys. Rev. B* **26**, 4269 (1982).
- [38] T. Uehlinger, G. Jotzu, M. Messer, D. Greif, W. Hofstetter, U. Bissbort, and T. Esslinger, *Phys. Rev. Lett.* **111**, 185307 (2013).
- [39] Z.-F. Xu, L. You, A. Hemmerich, and W. V. Liu, *Phys. Rev. Lett.* **117**, 085301 (2016).
- [40] L. Fu and E. Berg, *Phys. Rev. Lett.* **105**, 097001 (2010).
- [41] M. Sato, *Phys. Rev. B* **81**, 220504 (2010).
- [42] B. Mukherjee, Z. Yan, P. B. Patel, Z. Hadzibabic, T. Yefsah, J. Struck, and M. W. Zwierlein, *Phys. Rev. Lett.* **118**, 123401 (2017).
- [43] Y. Shin, C. H. Schunck, A. Schirotzek, and W. Ketterle, *Phys. Rev. Lett.* **99**, 090403 (2007).